Transport in Porous Media **38:** 223–240, 2000.

Laboratory, Field and Modeling Studies of Radon-222 as a Natural Tracer for Monitoring NAPL Contamination

LEWIS SEMPRINI*, OMAR S. HOPKINS and BRIAN R. TASKER
Department of Civil, Construction, and Environmental Engineering, Oregon State University, Corvallis, OR 97331-2302, U.S.A.

(Received: 9 September 1998)

Abstract. The recently developed natural radon tracer method has potential as a rapid, low-cost, nondestructive, and noninvasive method for quantifying NAPL contamination. In the subsurface, radon-222 (radon) is produced by the decay of naturally occurring radium-226 contained in the mineral fraction of aquifer solids. In groundwater radon occurs as a dissolved gas, with a half-life of 3.83 days. In the absence of NAPL, the radon concentration in groundwater quickly reaches a maximum value that is determined by the mineral composition of the aquifer solids, which controls the rate of radon emanation. In the presence of NAPL, however, the radon concentration in the groundwater is substantially reduced due to the preferential partitioning of radon into the organic NAPL phase. A simple equilibrium model and supporting laboratory studies show the reduction in radon concentration can be quantitatively correlated with residual NAPL saturation. Thus, by measuring the spatial distribution in radon it may be possible to identify locations where residual NAPL is present and to quantify the NAPL saturation. When the basic processes of partitioning, radon emanation from the aquifer solids, and first-order decay are incorporated into an advective/dispersive transport model, good agreement is obtained with the results of laboratory and field experiments. Model sensitivity analyses shows many factors can contribute to the radon concentration response, including the length of the NAPL zone, NAPL saturation, groundwater velocity, porosity, and radon emanation. Thus, care must be taken when applying the radon method to locate and quantify NAPL contamination in the subsurface.

Key words: NAPLs, radon, modeling, monitoring, partitioning, tracer, emanation.

Nomenclature

C_w	aqueous radon concentration [pCi/m^3].
C_n	NAPL radon concentration [pCi/m^3].
D	dispersion coefficient [m^2/h].
C_{Ra}	radium-226 concentration of the aquifer solids [pCi/kg].
E	radon emanation from source rocks [pCi/kg].
E_p	emanation power [-].
K_c	NAPL/water partition coefficient [pCi/m$^3{}_n$/pCi/m$^3{}_w$].
R	retardation factor [-].

* Author for correspondence: (tel.: (541)-737-6895; e-mail: lewis.semprini@orst.edu).

V darcy velocity [m/h].
S_w water saturation, volume water/ volume pore space [-].
S_n residual NAPL saturation, volume NAPL/volume pore space [-].

Greek Letters

ρ_b aquifer solids bulk density [kg/m^3].
ϕ aquifer porosity.
λ first-order radon decay coefficient [1/h].
α aquifer dispersivity [m].

1. Introduction

Successful remediation of NAPL contamination requires accurate estimation of the quantities of NAPLs present and their spatial distribution in the subsurface (Cohen and Mercer, 1993). The ability to monitor NAPL quantities during remediation activities is also desirable to quantify the extent of cleanup achieved and to verify the viability of the selected remedial technology. Existing methods for quantifying the extent and severity of NAPL contamination are limited by the complex nature of NAPL behavior and transport in the subsurface (Mercer and Cohen, 1990). For example, characterization of subsurface NAPL contamination by direct sampling is extremely expensive because of the typically 'patchy' nature of NAPL releases, the presence of heterogeneous subsurface materials, and the strongly directional nature of subsurface flow and transport processes. Thus, core samples must be collected in close proximity to the contaminated zones to yield representative and reliable results (EPA, DNAPL Workshop, 1992; Cohen and Mercer, 1993).

Recent research indicates that partitioning tracers can be reliably employed to detect and quantify NAPLs in the subsurface (Jin *et al.*, 1995; Nelson and Brusseau, 1996; Jin *et al.*, 1997). In a conventional partitioning tracer test, a prepared test solution containing a mixture of solutes is injected into a well in the saturated zone. The solutes are selected to have different affinities for the water and NAPL phases (e.g., anions and alcohols are more soluble in water than NAPL, while many organic acids, dyes, and dissolved gases are more soluble in NAPL than water). In a single-well test, the test solution/groundwater mixture is then pumped from the same well (Looney *et al.*, 1998); in a well-to-well test, the test solution/groundwater mixture is pumped from one or more downgradient wells (Jin *et al.*, 1997). In both types of tests, samples are analyzed to determine breakthrough curves for all solutes. The difference in arrival of the breakthrough curves at the well can be used to infer retardation factors and residual NAPL saturations if the NAPL/water partition coefficient is known for the partitioning tracer. Advantages of existing partitioning tracer tests are that they can utilize existing monitoring wells and are sensitive to the presence of small quantities of NAPL.

A new and potentially powerful partitioning tracer method for detecting and quantifying NAPL contamination is using naturally occurring radon-222 in subsurface samples (Semprini *et al.*, 1993, 1995, 1998; Hunkeler *et al.*, 1997). The method is based on detecting spatial or temporal changes in radon concentrations in groundwater samples. In the subsurface, radon-222 (radon) is produced by the decay of naturally occurring radium-226 contained in the mineral fraction of aquifer solids. In the saturated zone radon occurs as a dissolved gas, with a half-life of 3.83 days. In the absence of NAPL, radon concentrations in groundwater quickly reach a site-specific equilibrium (maximum) value that is determined by the mineral composition of the aquifer solids, which controls the rate of radon emanation. In the presence of NAPL, however, radon concentrations in groundwater can be substantially reduced due to the preferential partitioning of radon into the organic NAPL phase. Moreover, the reduction in radon concentration can be quantitatively correlated with the quantity of NAPL present in the pore space (Semprini *et al.*, 1993).

By measuring the spatial distribution in radon concentrations it may be possible to identify locations where NAPL is present and to predict residual NAPL saturation. Presented here are the results of laboratory and field observations and model simulations. A model sensitivity analysis illustrates the radon response to changes in NAPL saturation, groundwater velocity, length of the NAPL zone, and aquifer porosity.

2. Model Development

2.1. STEADY-STATE-RADON PARTITIONING MODEL

The natural radon tracer method is based on the partitioning of naturally occurring radon gas between the groundwater and NAPL phases. In the saturated zone, radon continuously emanates from the aquifer solids and enters the pore space. The rate of emanation is dependent on the concentration of radon in the source rock and the emanation power, which is the fraction of radon produced that enters the pore fluid. The equilibrium concentration of radon in the pore fluid is given by Andrews and Wood (1972):

$$C = \frac{C_{\mathrm{Ra}} E_{\mathrm{p}} \rho_{\mathrm{b}}}{\phi}, \tag{1}$$

where C is the radon concentration in the water (pCi/m^3), C_{Ra} is the radon concentration of the aquifer solids (pCi/kg), E_{p} is the emanation power, ρ_{b} is the bulk density (kg/m^3), and ϕ is the aquifer porosity. When NAPL is also present in the pore space, the radon will be present in both the water and the NAPL phases:

$$C_{\mathrm{n}} S_{\mathrm{n}} + C_{\mathrm{w}} S_{\mathrm{w}} = \frac{C_{\mathrm{Ra}} E_{\mathrm{p}} \rho_{\mathrm{b}}}{\phi}, \tag{2}$$

where C_{n} and C_{w} are the concentrations in the NAPL and water phases, respectively, and S_{n} and S_{w} are the NAPL and water phase saturations, respectively.

Assuming linear partitioning of radon between water and NAPL:

$$C_{\mathrm{n}} = K_{\mathrm{c}} C_{\mathrm{w}}, \tag{3}$$

where K_c is the water/NAPL partition coefficient, and C_w is the steady-state concentration of radon in water in the presence of NAPL

$$C_w = \frac{C_{Ra} E_p \rho_b / \phi}{1 + S_n (K - 1)}. \tag{4}$$

Equation (4) can be rearranged to give the deficit in radon concentration in the presence of NAPL:

$$\frac{C_{w(NAPL)}}{C_{w(background)}} = \frac{1}{1 + S_{NAPL}(K_C - 1)}, \tag{5}$$

where $C_{w(NAPL)}$ is the radon concentration (pCi/m^3) in a groundwater sample from the NAPL contaminated zone, $C_{w(background)}$ is the radon concentration (pCi/m^3) in a 'background' groundwater sample from outside the NAPL contaminated zone as given in Equation (1). The model represents conditions where the radon concentration in the water phase is in secular equilibrium with emanation from the aquifer solids, its own radioactive decay, and partitioning between phases. The model assumes the same mineralogy and radon emanation in the area of the background groundwater sample and for the area with NAPL contamination. The model predicts that as the residual NAPL saturation increases, radon concentrations in groundwater within the NAPL contaminated zone decrease compared to radon concentrations in background samples. We will call this decrease the 'radon deficit'.

Few values for radon NAPL/water partition coefficients exist in the literature for NAPLs of environmental concern. Based on literature values of radon solubility, normally given as Ostwald solubility coefficients, the partition coefficient, K_c is expected to range from 20 to 80 for most NAPLs, based on data compiled by Clever (1979). Ostwald solubility coefficients and the estimated K_c values obtained by dividing the organic Oswald coefficient by the water coefficient are provided in Table I. Potential LNAPLs (Benzene, Toluene, Xylene, Hexane) have similar K_c values ranging from 45 to 58, while those for DNAPLS ($CHCl_3$ and CS_2) have K_c values of 53 and 81, respectively. Thus, a DNAPL, such as trichloroetheylene (TCE) is expected to have a high partition coefficient, similar to chloroform ($CHCl_3$).

Equilibrium partitioning model predictions based on Equation (5) are presented Figure 1, where the theoretical Rn deficit is plotted versus the percentage residual NAPL saturation as a percent of the pore space. The radon deficit is extremely sensitive to the presence of small residual NAPL saturations. For a K_c value of 50, the estimated value for a chlorinated solvent ($CHCl_3$, Table I), a residual saturation of only 1%, results in a 33% reduction in the aqueous radon concentration. The response is nonlinear with respect to NAPL saturation with the greatest radon signal changes occurring as the residual NAPL saturation approaches zero. The method is not sensitive at high values of NAPL saturation. This simple equilibrium model indicates how measured radon concentration might be used to quantify residual NAPL saturation and monitor changes in residual saturation as remediation

Table I. Oswald coefficients (Cleaver, 1979) and estimated organic-water partitioning coefficients for radon-222

Compound	Ostwald coefficient (L)	Partition coefficient (K_c)
Water	0.285	–
CS_2	23.14	81
$CHCl_3$	15.08	53
Benzene	12.82	45
Toluene	13.24	46
Hexane	16.56	58
Xylene	15.4	54
Di-ethyl-ether	15.08	53
Petroleum	9.01	32
1-Pentanol	10.6	37
2-Butanol	7.58	26
Methanol	5.4	19

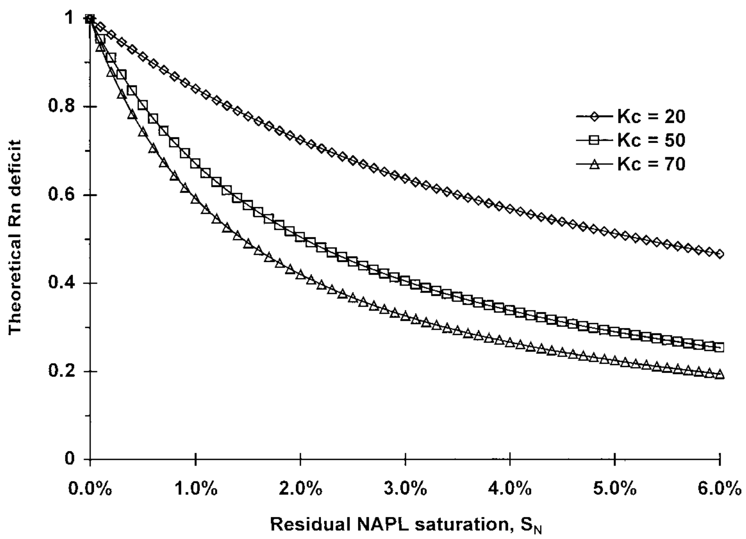

Figure 1. Theoretical radon deficit for several values of the NAPL/water Rn Partition Coefficient, K_c.

proceeds. Due to it's short half-life of 3.83 days, and constant rate of emanation from the aquifer solids, the radon concentration in the pore fluids would rapidly equilibrate to changes of NAPL saturation as remediation proceeds over times scales of months to years.

2.2. ONE-DIMENSIONAL MODEL FOR RADON TRANSPORT WITH NAPL PARTITIONING

The ability of the radon tracer method to identify and quantify residual NAPL saturations in the subsurface is illustrated with simulations using a one-dimensional flow and transport model. Hunkler *et al.* (1997) used a similar model formulation to establish steady-state concentrations provided in Equation (5), under flow conditions. The model presented here, originally presented by Tasker (1995), was used as the basis of a one-dimensional numerical transport code. The model includes terms for radon emanation from aquifer solids, radon radioactive decay, advective and dispersive transport of radon by groundwater flow, and equilibrium partitioning between the stationary residual NAPL phase and the mobile groundwater phase. The model is similar in construct to models used for partitioning tracers (Nelson and Brusseau, 1996), but terms are added for radon emanation from the aquifer solids and first-order radon decay.

The single-phase radon transport model includes properties of radon's emanation source and radioactive decay in addition to the more classical transport properties of dispersion and advection. This equation is given by (Clements and Wilkening, 1974):

$$\frac{\partial(\phi C)}{\partial t} = \underbrace{\frac{D\phi\partial^2 C}{\partial x^2}}_{\text{(dispersion)}} - \underbrace{\frac{\partial(VC)}{\partial x}}_{\text{(advection)}} - \underbrace{\lambda\phi C}_{\text{(decay)}} + \underbrace{E\rho_\mathrm{b}\lambda}_{\text{(emanation)}}, \tag{6}$$

where E represents the radium concentration of the aquifer solids times the emanation power ($C_\mathrm{Ra} \times E_\mathrm{p}$), D is the dispersion coefficient (m^2/h), V is the darcy velocity (m/h), and λ is the first-order decay rate for radon (0.00754 h^{-1}). This model assumes that the radon emanation, E, is constant and independent of the radon concentration in the pore fluid, which is a reasonable based on radon emanation theory (Tanner, 1978; Fleischer, 1983).

The two-phase radon transport model also includes properties of radon's NAPL/water partitioning. This is accomplished by differentiating between radon concentrations in the aqueous and NAPL phases:

$$\begin{aligned}\frac{\phi\partial(C_\mathrm{w}S_\mathrm{w} + C_\mathrm{n}S_\mathrm{n})}{\partial t} = {} & \frac{D\phi S_\mathrm{w}\partial^2 C_\mathrm{w}}{\partial x^2} + \frac{D\phi S_\mathrm{n}\partial^2 C_\mathrm{n}}{\partial x} - \frac{\partial(C_\mathrm{w}V_\mathrm{w})}{\partial x} - \\ & - \frac{\partial(C_\mathrm{n}V_n)}{\partial x} - \lambda\phi C_\mathrm{w}S_\mathrm{w} - \lambda\phi C_\mathrm{n}S_\mathrm{n} + E\rho_\mathrm{b}\lambda. \end{aligned} \tag{7}$$

The model assumes that emanation is independent of the pore fluid saturation, which is also reasonable based on radon emanation theory. For example, the same radon emanation rate was observed into pores filled with either water or moist air (Tanner, 1978; Thamer *et al.*, 1982).

Assuming that the NAPL phase is immobile, the two-phase radon transport equation reduces to

$$\frac{\phi\partial(C_\mathrm{w}S_\mathrm{w}+C_\mathrm{n}S_\mathrm{n})}{\partial t} = \frac{D\phi S_\mathrm{w}\partial^2 C_\mathrm{w}}{\partial x^2} - \frac{\partial(C_\mathrm{w}V_\mathrm{w})}{\partial x} - \\ -\lambda\phi C_\mathrm{w}S_\mathrm{w} - \lambda\phi C_\mathrm{n}S_\mathrm{n} + E\rho_\mathrm{b}\lambda \tag{8}$$

Assuming equilibrium partitioning is achieved, and the local equilibrium assumption applies, the partitioning equation is substituted for C_n in the two-phase radon transport equation to give the following expression after rearrangement:

$$\left(1+\frac{K_\mathrm{c}S_\mathrm{n}}{S_\mathrm{w}}\right)\frac{\partial C_\mathrm{w}}{\partial t} = \frac{1}{S_\mathrm{w}\phi}\left[\frac{D\phi S_\mathrm{w}\partial^2 C_\mathrm{w}}{\partial x^2} - \frac{\partial(C_\mathrm{w}V_\mathrm{w})}{\partial x} + E\lambda\rho_\mathrm{b}\right] - \\ -\lambda C_\mathrm{w}\left(1+\frac{K_\mathrm{c}S_\mathrm{n}}{S_\mathrm{w}}\right). \tag{9}$$

The equation also assumes that the residual NAPL saturation does not change (i.e. the NAPL is not slowly dissolving). Due to the short half-life of radon, this is a reasonable assumption for the short-term simulations of 1 month or less that are required to achieve steady-state spatial distributions. The retardation factor is represented by

$$R = 1+\frac{K_\mathrm{c}S_\mathrm{n}}{S_\mathrm{w}}. \tag{10}$$

After substitution for R and rearrangement, the aqueous phase radon transport in saturated soil equation can be expressed as

$$\frac{\partial C_\mathrm{w}}{\partial t} = \frac{1}{S_\mathrm{w}\phi R}\left[\frac{D\phi S_\mathrm{w}\partial^2 C_\mathrm{w}}{\partial x^2} - \frac{\partial(C_\mathrm{w}V_\mathrm{w})}{\partial x} + E\lambda\rho_\mathrm{b}\right]\lambda C_\mathrm{w}. \tag{11}$$

The final form of this equation is similar to that given by Nelson and Brusseau (1996), for partitioning tracers, with additional terms for radon emanation and first-order decay. Equation (5) can be derived from Equation (11) with the assumption of steady-state conditions and no flow. If the NAPL zone has sufficient length, the steady-state solution of Equation (11) will yield Equation (5) with flow occurring (see Hunkeler *et al.*, 1997 for the mathematical derivation).

This Equation (11) was solved numerically using the finite difference method. The numerical solution was tested with analytical solutions to (1) the advective/dispersion equation (Van Genuchten, 1981), (2) the steady-state radon transport equation with advection, first-order decay, and constant emanation source term (Clements and Wilkening, 1974), and the steady-state solution to Equation (5) (Tasker, 1995).

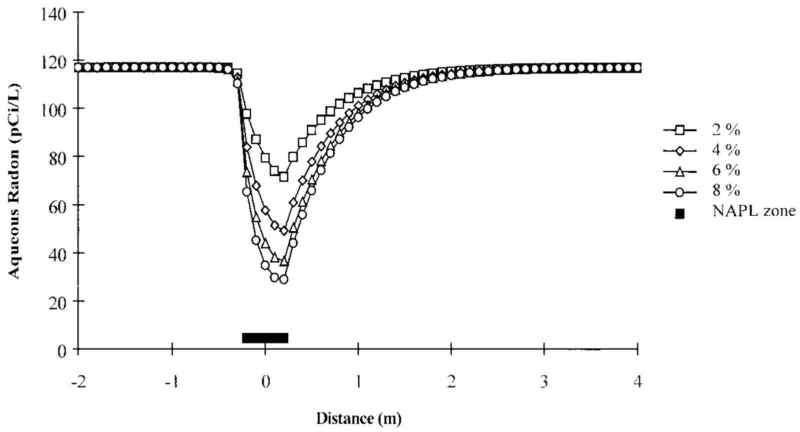

Figure 2. One-dimensional model simulations of the steady-state radon concentration profile upgradient, within and downgradient of a uniformly distributed residual NAPL zones. Simulations are presented for NAPL saturations of 2%, 4%, 6% and 8%.

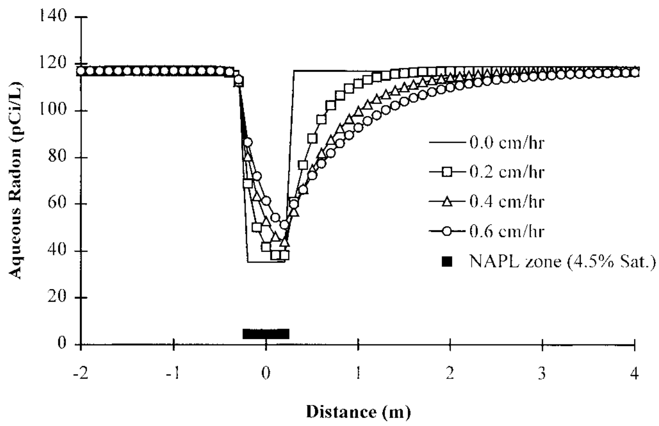

Figure 3. One-dimensional model simulations of the steady-state radon concentration profiles upgradient, within, and downgradient of a uniformly distributed residual NAPL zone with a saturation of 4.5%. Simulations are presented for pore water velocities of 0, 0.2, 0.4, and 0.6 cm/h.

2.3. ONE-DIMENSIONAL MODEL SIMULATIONS

One-dimensional model simulations presented in Figures 2–5 illustrate the radon concentration response as groundwater flows through a zone of residual NAPL contamination that is uniformly distributed over 0.5 m of porous media. Model input parameters are provided in Table II. Figure 2 shows the steady-state spatial distribution of groundwater radon concentrations for simulations performed with different degrees of residual saturation. The upgradient radon concentration is in equilibrium with emanation from the aquifer solids in the absence of residual NAPL, based on Equation (1). The model simulations clearly show the reduction in radon concentration that occurs as groundwater flows through the NAPL con-

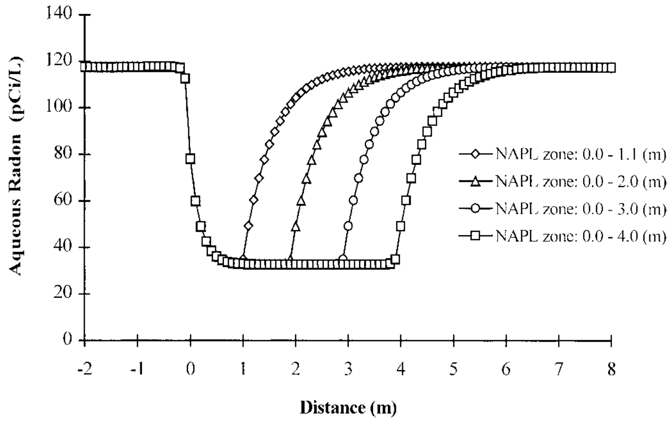

Figure 4. One-dimensional model simulations of the steady-state radon concentration profiles upgradient, within, and downgradient of a uniformly distributed residual NAPL zone with a saturation of 4.5%. Simulations are presented for NAPL zones having lengths of 1, 2, 3, and 4 m.

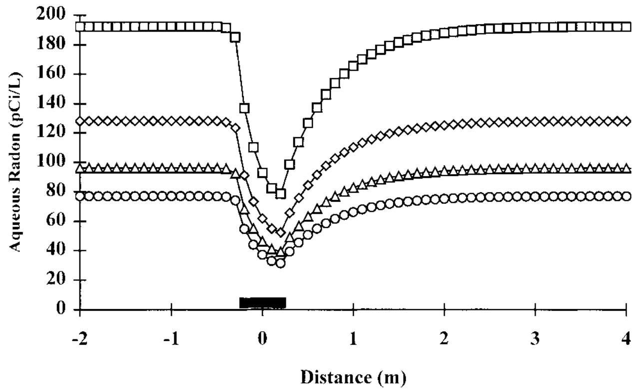

Figure 5. One-dimensional model simulations of the steady-state radon concentration profiles upgradient, within, and downgradient of a uniformly distributed residual NAPL zone with a saturation of 4.5%. Simulations are presented for aquifers with porosities of 0.2, 0.3, 0.4, and 0.5. The radon concentration increases as porosity decreases.

taminated zone. As expected, the magnitude of the decrease is correlated to the NAPL residual saturation. As groundwater leaves the NAPL contaminated zone, the radon concentration gradually returns to background levels due to continued radon emanation from the aquifer solids. Only a short distance of travel is required for the re-equilibration to occur due to the short half-life of radon (3.83 days) relative to the pore water velocity. The distance required for the radon concentration to return to background levels is also dependent on the quantity of NAPL present, due to the reduction in radon concentration. The simulations show that the radon deficit signal is not carried a great distance from the NAPL zone. Thus, the ability to detect NAPL contamination is restricted to locations close to the NAPL zone.

Table II. Parameters used in the model simulations

Parameter	Figures 2–5	Figure 6	Figure 7	Figure 8
C_{in}(pCi/l)[a]	117	0	117	20
E (pCi/g)	0.0251	0.043	0.024	0.0295
K_c(-)	50	38	50	50
V (cm/h)[b]	0.132[c]	16.4	0.113	0.137
S_n (%)	4.47[d]	0, 1.0, 5.0	4.47	7.55
ϕ (-)	0.33[e]	0.41	0.33	0.33
ρ_b(g/l)	1691	1691	1691	1691
α (cm)	5.8	0.72	5.8	5.8
Length NAPL (cm)	50[f]	Total Column	50	50

[a]Influent concentration. [b]Darcy velocity.
[c]varies in Figure 3. [d]varies in Figure 2. [e]varies in Figure5. [f]varies in Figure 4.

Shown in Figure 3 are model simulations conducted with a range of groundwater velocities and at a residual saturation of 4.5%. Increasing the groundwater velocity results in decreased radon concentration deficit profiles in the NAPL zone and an increased distance downstream to reestablish the equilibrium concentration. The maximum deficit of radon does not occur at the higher groundwater velocities due to the more rapid transport through the NAPL zone.

The establishment of a maximum deficit is illustrated in Figure 4, which shows the aqueous radon concentration as a function of NAPL zone length. Increasing the NAPL zone length results in the establishment of a sustained maximum deficit concentration. The steady-state aqueous radon concentration is reduced to 29% of the upgradient value, which agrees with the value of 31% predicted by Equation (5) for the K_C and saturation values used in the transport simulations.

Figure 5 shows how changes in porosity would effect the radon concentration profiles. As Equation (1) predicts, in the absence of NAPL, a decrease in porosity would result in higher radon concentrations in the pore fluid. Thus, variability in aquifer porosity is one of the geologic parameters that can complicate the interpretation of radon concentration measurements for locating NAPL contamination. Similar results would be obtained by changing the emanation source term.

2.4. COMPARISON OF MODEL SIMULATIONS WITH THE RESULTS OF LABORATORY COLUMN EXPERIMENTS

Model simulations are compared with the results of laboratory column studies conducted by Hopkins (1994). Column studies were performed using natural radon emanating from aquifer solids to correlate the radon deficit with the degree of NAPL saturation, and to study radon transport as a function of residual NAPL saturation. The columns were packed with aquifer solids from the CFB Borden test site in Ontario, Canada. The NAPL chosen for the studies was Soltrol 220® (Soltrol) (Phillips Petroleum). The water–Soltrol interfacial tension was reduced by the addition of 0.5% by weight Lubrizol™ (McBride *et al.*, 1992). This altered the Soltrol from a non-spreading fluid to a highly spreading fluid on water and immobilized the Soltrol on the Borden sand. This modification permitted the construction of soil columns with residual saturations ranging from 0% to 8%. Glass columns (1060 ml) with a pore volume of 445 ml (porosity of 0.42) were packed with Borden aquifer solids wet with the desired degree of NAPL residual saturation. After packing, the columns were saturated with gas-free water and allowed to equilibrate for 2–4 weeks under no flow (static) conditions. This permitted the radon concentrations in the pore fluids to reach secular equilibrium with emanation from the aquifer solids. The columns were then exchanged over a period of several hours, by exchanging variable pore volumes of radon-free water. The radon concentration in the groundwater exiting the column was measured as a function of the pore volume exchanged. The radon concentration was measured as described by Lucas (1964). Hopkins (1994) provides a detailed description of these experiments.

Numerical simulations were performed for each column test. The simulations consisted of a 2–4 weeks period with no flow (time depending on that of the real test) followed by the dynamic exchange, where groundwater-lacking radon was flushed through the column. The dispersivity, α, was determined by fitting the breakthrough curve for 0% NAPL saturation. A best-fit partition coefficient, K_c, of 38 was used for Soltrol based on the results of Hopkins (1994). This value is in the range of petroleum compounds (Table I). Parameters used in the simulations are provided in Table II.

The simulation and the experimental results for three different NAPL saturations (0%, 1%, and 5%) are presented in Figure 6. In general, the simulations agree well with the experimental data. As the saturation increases, the maximum radon concentration (equilibrated pore fluid) decreases, as expected based on Equation (5). The volume of water exchanged to achieve the breakthough of radon-free groundwater also increases due to the retarded transport, as expected based on Equation (10).

Figure 6(A) presents the results for 0% NAPL saturation. The maximum simulated aqueous radon is 160 pCi/l, while the measured is 173 pCi/l. The groundwater concentration exiting the column is reduced to the minimum equilibrium concentration of 3 pCi/l after an exchange of approximately 750 ml of radon-free groundwater. The 50% breakthough concentration occurs after 445 ml of groundwater is exchanged, consistent with a measured pore volume of 443 ml. Thus no retardation was observed, which is consistent with no NAPL being present.

Figure 6(B) shows the results for the column with a residual NAPL saturation of 1%. The maximum measured radon concentration is reduced to 121 pCi/l, and the simulated maximum value is 112 pCi/l. Both the measured and simulated maximum values represent 70% of the 0% NAPL saturation case. This reduction is in good agreement with the value of 73% obtained by using Equation (5). Both the

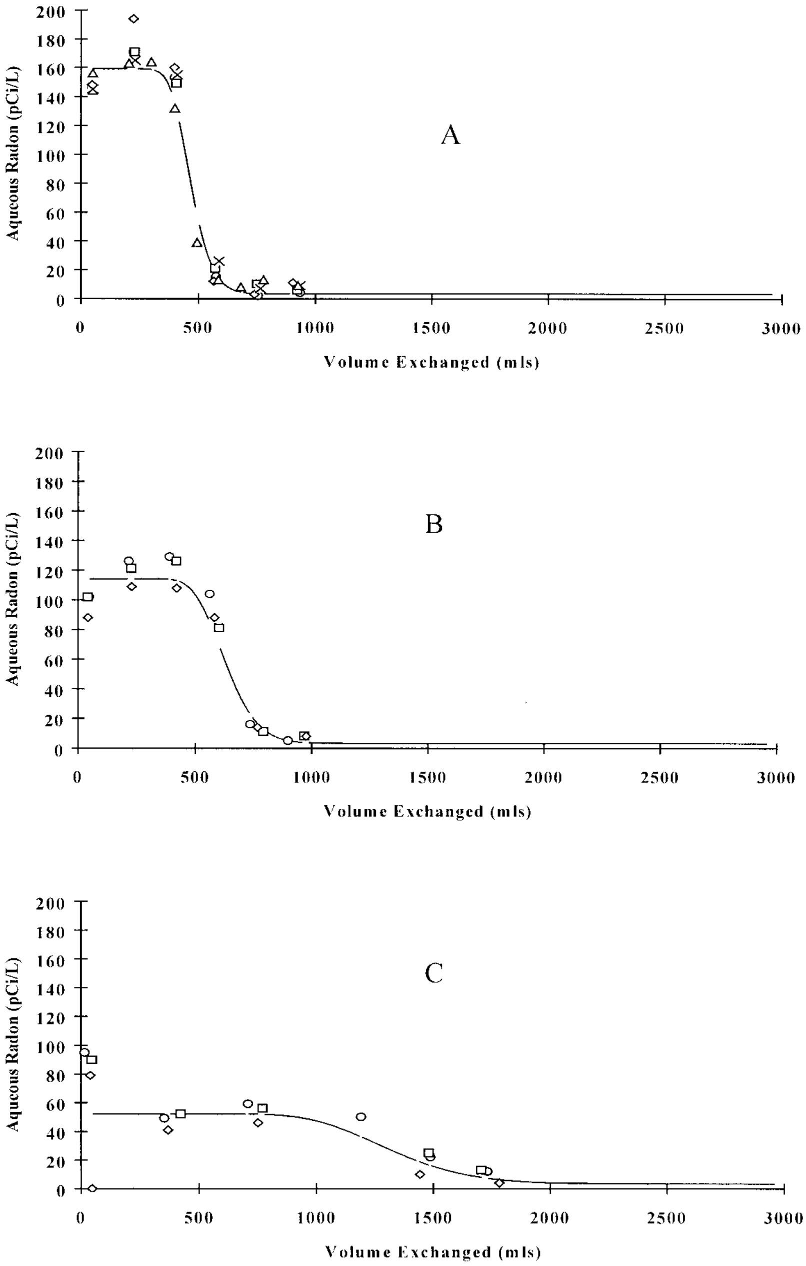

Figure 6. Exit radon concentrations from soil columns during the exchange of radon equilibrated pore water with groundwater lacking radon: (A) 0% residual NAPL saturation; (B) 1% residual NAPL saturation; (C) 5% residual NAPL saturation.

experiments and the simulations also show an increase in the volume of exchange water required to achieve low radon values due to the retarded transport. The experimental retardation factor of 1.44 is in close agreement with the value of 1.38 obtained by using Equation (10), and is used in the model simulations. Figure 5C presents results for the 5% residual saturation case. The maximum measured radon concentrations of both the experimental and simulated columns were reduced to 31% of the 0% NAPL saturation case, compared with an estimate of 35% based on Equation (5). The retardation factor of 3.2 agrees with the value of 3.0 used in the model simulations (Equation (10)). Experimental and simulation results for column studies performed at residual saturations 2.5% and 8% (not shown) compared equally well as those described above.

Our results are in good agreement with those of Hunkeler *et al.* (1997) who performed batch partitioning experiments that showed a good agreement between experimental results and Equation (5). The column results and nonsteady-state simulations presented here illustrate the retarded radon transport due to the presence of NAPL, and the radon deficits that result from the presence of NAPL. Our experimental data showed some discrepancies from radon concentrations predicted at low values of the volume water exchanged. This was most likely due to 'column end effects' associated with the experimental procedures used in packing the columns as described by Hopkins (1994). The results, however, show the basic partitioning, and transport processes predict well the radon response for these simple cases. In these experiments the NAPL was made to wet the aquifer solids. This likely resulted in the development of large interfacial surface areas and rapid mass transfer. Thus, the assumption of equilibrium partitioning appeared to be met for the experimental cases that were simulated.

2.5. COMPARISON OF MODEL SIMULATIONS TO THE BORDEN AQUIFER TESTS

The radon method was investigated in two controlled field studies conducted at the CFB Borden test site in Ontario, Canada. In the first study, a fairly uniform NAPL source, composed of a mixture of chloroform, trichloroethylene, and tetrachloroethylene, was emplaced in the shallow sand aquifer and permitted to slowly dissolve under natural gradient groundwater flow conditions (Rivett, 1995; Feenstra, 1997; Feenstra and Cherry, 1998). The experiment represents conditions of a very well distributed DNAPL source. During the course of this experiment groundwater samples for radon measurement were obtained from three locations: upgradient, within, and downgradient of the NAPL source. Replicate samples were obtained from each location over a period of several months. The radon concentration in the NAPL zone decreased by a factor of 2–3 from the values observed upgradient for each sampling event (Figure 7). The radon concentration downgradient of the NAPL source reequilibrated within a few meters to the upgradient value, indicating that the radon deficit is limited to the portion of the aquifer nearest to the source.

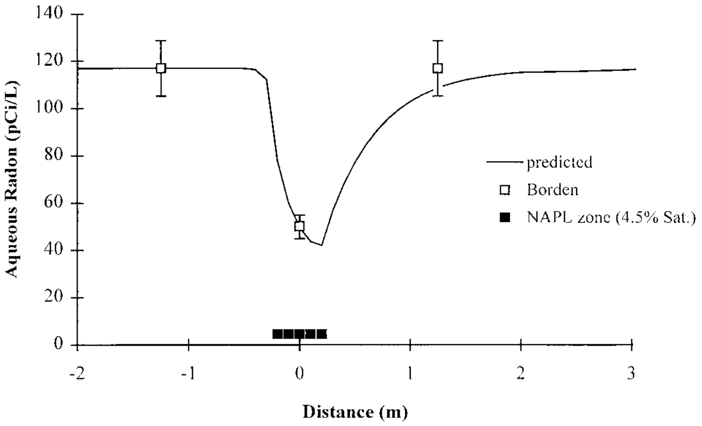

Figure 7. Spatial groundwater radon concentrations and steady-state one-dimensional model simulations of the 'emplace source' experiment conducted at the Borden test site with groundwater flowing under natural gradient conditions. Error bars represent variations observed in three radon surveys.

One-dimensional model simulations were performed using transport parameters for the Borden aquifer in the region of the test (Rivett, personnel communication). The results of these model simulations and predicted radon concentrations are shown in Figure 7. The model simulation's changes in spatial concentrations are similar to those observed in the aquifer. A NAPL residual saturation of 4.5% was used in the model simulations to achieve the response shown. A partition coefficient of 50 was selected based on literature values for chloroform ($CHCl_3$), which was one of the components of the NAPLs in the source zone. The NAPL saturation emplaced in the aquifer was approximately 3.8% (Rivett, personnel communication). Although the number of spatial radon measurements is limited, the agreement between the radon method and emplaced saturation is quite encouraging. It is interesting to note that at the groundwater flow velocity of 9.7 cm/day the simulated radon concentration rapidly reequilibrated to upgradient field observations. The results further demonstrate the radon deficit occurs only very close to the NAPL contamination.

The second experiment referred to as the 'free-release' experiment involved the injection of 5 l of NAPL into a sand aquifer inside a steel-sheet-pile test cell (Feenstra, 1997; Feenstra and Cherry, 1998). The NAPL was permitted to distribute itself in the aquifer and form an irregular NAPL zone (Fennstra and Cherry, 1998). Groundwater flow was induced by injecting and pumping groundwater at the ends of the cell; the induced groundwater velocity within the test cell was 10.1 cm/day. The radon-stripped recharge water (with a maximum 20 pCi/l radon concentrations) was continuously injected upstream from the NAPL zone. In order for a steady-state radon concentration distributions to be achieved, measurements were made after 1 month of induced flow conditions. Three surveys were performed all showing nearly identical steady-state spatial distributions.

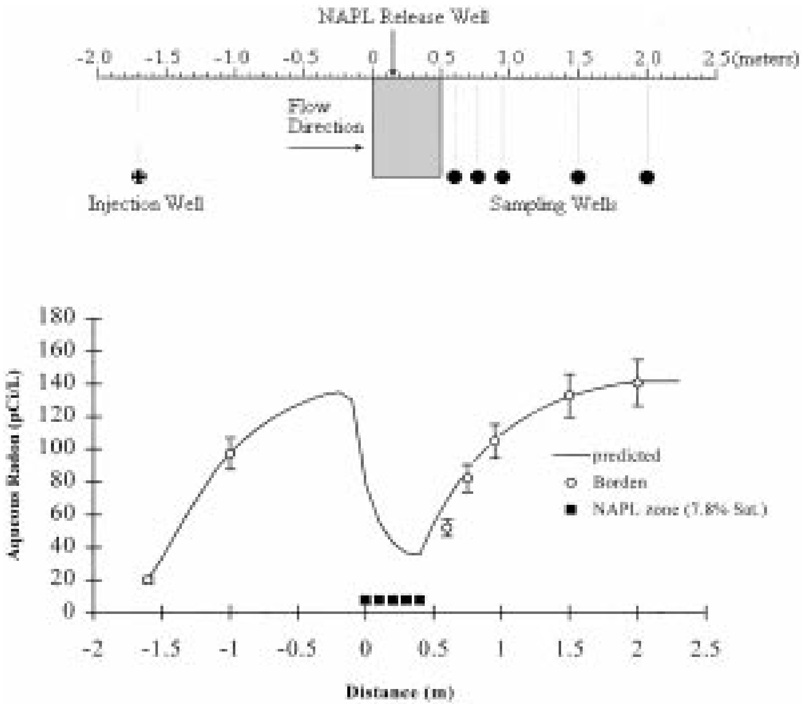

Figure 8. Sampling locations and the spatial radon concentrations and steady-state simulation results for the 'free release' NAPL test at the Borden test site. One-dimensional simulations were performed with a 0.5 m source zone having a NAPL saturation of 7.8%. Error bars represent variations observed in three radon surveys.

A schematic of the recharge experimental layout is shown in Figure 8 along with the measured radon concentrations and model predictions. The measured radon concentrations and model predictions indicate a zone of NAPL contamination in the region of approximately 0 – 0.5 meters, and the likely absence of NAPL at the same depth, downgradient of this location. A residual NAPL zone 0.5 m in length when combined with a residual saturation of 7.8% produced a radon concentration profile that matched the field measurements. These values were obtained by trial and error, and represent just one combination of NAPL size and residual saturation that can produce the spatial radon distribution observed. For example, as shown in Figure 4, a response similar to that observed could be achieved with a source zone 1 m long and a residual saturation of 4.5%. Despite the limited spatial resolution, the combined modeling and field results indicate NAPL contamination exists at the depth interval of sampling at a spatial location near 0 and 0.5 m. The presence of NAPL in this location was confirmed when the contaminated zone was excavated (Broholm, personel communication).

3. Summary

Both laboratory and field experimental results, combined with the radon transport modeling support the proposed method of using naturally occurring radon-222 to locate and quantify NAPL contamination. The transport model, although developed with many simplifying assumptions, consistently produced results that agreed with experimental data from both the laboratory and the field. Some general trends regarding aqueous radon concentration profiles in the presence of NAPL have been established. Aqueous radon concentrations decrease relative to background when NAPL is encountered, creating a radon deficit. The radon deficit increases as NAPL saturation increases. When a sufficiently long zone of well-distributed NAPL zone is present the aqueous radon can achieve a maximum deficit governed by the partitioning relationship given in Equation (5).

Aqueous radon concentrations are affected by the presence of NAPL in the direct proximity of the NAPL zone. In most groundwater flow situations the signal will be propagated, at most, only a few meters from the source zone. An exception would involve conditions of high groundwater velocities. This short propagation of the radon signal likely limits radon as an exploratory method for locating NAPL contamination. It, however, provides a method for defining NAPL contamination over short spatial intervals.

Precautions must be taken when applying this method in practice. Heterogeneities in aquifer porosity and radon emanation will have a major impact on measured radon concentrations. Thus, the application of this method needs to consider potential geologic variability. The best results will likely be obtained in fairly homogenous aquifers, or locally where the subsurface geology does not change. Semprini *et al.* (1998) indicates the method has potential for monitoring the progress of NAPL remediation. Here the subsurface geology will likely remain constant as remediation proceeds. Radon concentrations in groundwater should increase as NAPL is removed by remediation, and thus the progress of remediation might be tracked. Development of radon transport models that permit the saturation to change temporally and spatially as remediation proceeds are needed.

The results also indicate how both the deficit in radon concentration and the transport of radon might be used to investigate NAPL contamination. The column exchange experiments illustrate the usefulness of radon as an *in situ* tracer. The retardation response can be monitored by injecting groundwater that lacks radon into the aquifer. Tests might be performed by injecting a conservative tracer, such as bromide, along with radon free groundwater. The retarded breakthrough in radon free water at surrounding monitoring wells might serve as an indicator of NAPL contamination. Here the transport time from the injection well to the monitoring well needs to be short (on the order of a few days or less) so significant changes in radon concentration do not result from emanation from the aquifer solids. The radon method could easily be incorporated and complement conventional partitioning tracers that are added. The potential benefit of radon is that it is always present, and need not be added. Thus, in some cases, only the monitoring of radon needs to be performed.

Acknowledgements

The authors wish to acknowledge Kim Broholm and Michael McDonald for their help in conducting the Borden Field experiments and the University Consortium Solvents-In-Groundwater Research Programme for access to the Borden Field experiments. This research was funded through a grant from the US EPA's Sponsored Western Region Hazardous Substance Research Center, under agreement R-815738 and a grant through the Department of Energy's Environmental Management Science Program. The article has not been reviewed by these agencies, and no official endorsement should be inferred.

References

Andrews, J. N. and Wood, D. F.: 1972, Mechanisms of radon release in rock matrices and entry into groundwater, *Inst. Mining and Metallurgy Trans*. **81**, B198–B209.

Clements, E. W. and Wilkening, M. H.: 1974, Atmospheric pressure effects on radon-222 transport across the earth–air interface, *J. Geophys. Res.* **79**(33), 5025–5029.

Clever, L. H. (ed.): 1979, *Krypton, Xenon, and Radon-Gas Solubilities*, Solubility Data Series 2, Vol. 18, Pergamon, New York.

Cohen, R. M. and Mercer, J.W.: 1993, *DNAPL Site Evaluation*, CRC Press, Boca Raton, Florida.

Environmental Protection Agency: 1992, Dense nonaqueous phase liquids: a workshop summary, In: *Dense Nonaqueous Phase Liquids*, Dallas, Texas, EPA, p. 81.

Feenstra, S.: 1997, Aqueous concentration ratios to estimate mass of multi-component NAPL residual in porous media, PhD Thesis, Department of Earth Sciences, University of Waterloo, Ontario, Canada.

Feenstra, S. and Cherry, J. A.: 1998, Aqueous concentration ratios to estimate mass of multi-component NAPL residual, In: G. B. Wickramamayake and R. E. Hinchee (eds), *Nonaqueous-Phase Liquids: Remediation of Recalcitrant Compounds*, Battelle Press, Columbus, OH, pp. 55–60.

Fleischer, R. L.: 1983, Theory of alpha recoil effects on radon release and isotopic disequilibrium, *Geochim. Cosmochim. Acta* **47**, 779–784.

Jin, M., Buler, R. E., Jackson, R. E., Mariner, P. E., Pickens, J. F., Pope, G. A., Brown, C. L. and McKinney, D. C.: 1997, Sensitivity models design and protocol for partitioning tracers in alluvial aquifers, *Ground Water* **35**(6), 964–972.

Jin, M., Delshad, M., Dwarakanath, V., McKinney, D. C., Pope, G. A., Sepehroori, K. and Tilburg, C. E.: 1995, Partitioning tracer test for detection, estimation, and monitoring the remediation performance assessment of subsurface nonaqueous phase liquids, *Water Resour. Res.* **31**(5), 1201–1211.

Van Genuchten, M.: 1981, Analytical solutions for chemical transport with simultaneous adsorption, zero-order production, and first-order decay, *J. Hydrol.* **49**, 213–233.

Hunkeler, D., Hoehn, E., Hohener, P. and Zeyer, J.: 1997, ^{222}Rn as a partitioning tracer to detect diesel fuel contamination in aquifer: laboratory study and field observations, *Environ. Sci. Technol*. **31**(11), 3180–3187.

Hopkins, O. S.: 1994, Radon-222 as an indicator for nonaqueous phase liquids in the saturated zone: developing a detection technology, Master's Thesis, Oregon State University.

Looney, B. B, Jerome, K. M. and Davey, C.: 1998, Single-well DNAPL characterization using alcohol injection/extraction, In: G. B. Wickramamayake and R. E. Hinchee (eds), *Nonaqueous-Phase Liquids: Remediation of Recalcitrant Compounds*, Battelle Press, Columbus, OH, pp. 55–60.

Lucas, H. F.: 1964, A fast and accurate survey technique for both ^{222}Rn and ^{226}Ra, In: J. A. S. Adams and W. M. Lowder (eds), *The Natural Radiation Environment*, Chicago, Illinois, University of Chicago Press, p. 315.

McBride, J. F., Simmons, C. S. and Cary, J. W.: 1992, Interfacial spreading effects on one-dimensional organic imbibition in water-wetted porous media, *J. Contam. Hydrol.* **11**, 1–25.

Mercer, J. and Cohen, R.: 1990, A review of immiscible fluids in the subsurface, *J. Contam. Hydrol.* **6**, 107–163.

Nelson, N. T. and Brusseau, M. L.: 1996, Field study of partitioning tracer method for detection of dense nonaqueous phase liquid in a trichloroethene-contaminated aquifer, *Eviron. Sci. Technol.* **30**(9), 2859–2863.

Rivett, M. O.: 1995, Soil gas signatures from volatile chlorinated solvents: Borden Field experiments, *Ground Water* **33**(1), 84–98.

Semprini, L., Broholm, K. and McDonald, M.: 1993, Radon-222 deficit method for locating and quantifying NAPL contamination in the subsurface, *EOS Trans. American Geophys. Union* **74**(43), 299.

Semprini, L., Hopkins, O. S., Gottipati, S. and Tasker, B. R.: 1995, Field, laboratory and, modeling studies of radon-222 as a natural tracer for detecting NAPL contamination in the subsurface and monitoring the progress of remediation, *EOS Trans. American Geophys. Union* **76**(46), F276.

Semprini, L., Cantaloub, M., Gottipati, S., Hopkins, O. and Istok, J.: 1998, Radon-222 as a tracer for quantifying and monitoring NAPL remediation, In: G. B. Wickramamayake and R. E. Hinchee (eds), *Nonaqueous-Phase Liquids: Remediation of Recalcitrant Compounds*, Battelle Press, Columbus, OH, pp. 137–142.

Tanner, A. B.: 1978, Radon migration in the ground: a supplementary review. In: T. Gessel and W. Lowder (eds), *The Natural Radiation Environment III*, Department of Energy, Oak Ridge, TN, pp. 5–56.

Tasker, B. R.: 1995, Radon-222 as an indicator for a nonaqueous phase liquids in the saturated zone: a numerical methods analysis, Engineering Report, MS Degree, Department of Civil Engineering, Oregon State University.

Thamer, B. J., Nielson, K. K. and Felthauser, K.: 1982, The effect of moisture on radon emanation including the effects of diffusion, Bureau of Mines Open File Report No. 184–84.